Research Article   Open Access

A Facile Electrochemical Sensor Based on Synergic Effect Strategy of poly(L-cysteine) and rGO-AgNPs Network for Highly Sensitive Detection of Metronidazole

Yexuan Mao, Mingyue Ding, Meng Dang, Xianqing Huang, Mingwu Qiao, Lianjun Song, Youyi Wang, Zizhe Li, Ke Song and Xiya Zhang[*]

Henan Province Engineering Research Center for Food Safety Control of Processing and Circulation, College of Food Science and Technology, Henan Agricultural University, Nongye Road, Zhengzhou, Henan, PR China

[*]Corresponding author: Xiya Zhang, Henan Province Engineering Research Center for Food Safety Control of Processing and Circulation, College of Food Science and Technology, Henan Agricultural University, Nongye Road, Zhengzhou, Henan 450002, PR China, Tel: +86-0371-6355 8150, E-mail: zhangxiya@henau.edu.cn

Citation: Yexuan Mao (2022) A Facile Electrochemical Sensor Based on Synergic Effect Strategy of poly(L-cysteine) and rGO-AgNPs Network for Highly Sensitive Detection of Metronidazole. J Nanotech Smart Mater 8: 1-14.

Abstract

Reduced graphene oxide-silver nanoparticles (rGO-AgNPs) composites have good catalysts and electrical conductivity. Herein, based on rGO-AgNPs modified glassy carbon electrode (GCE), a highly sensitive electrochemical sensor is developed for rapid detection of metronidazole (MNZ). The rGO-AgNPs nanoparticles were first synthesized by one-pot green synthesis method using the amino acid L-cysteine (L-cys) as the reductant. L-cys was considered as a weak reductant to reduce GO and AgNO3, as well as a linker agent to disperse and immobilize the AgNPs loaded stably on the graphene to prevent the aggregation of bulk-quantity rGO nanosheets caused by strong π-π stacking in different nanosheets, simultaneously. Poly(L-cys) obtained by electropolymerization, was synergized with rGO-AgNPs nanocomposites to enhance electrocatalytic effects for the detection of MNZ. Under the optimal experimental conditions, the detection limit of the sensitive electrochemical sensor in milk samples was 0.4 ng mL^{-1}. The recovery was ranged from 88.4% to 106.8% with relative standard deviation (RSD) below 5.1 %. Thus, this method developed here was suitable for MNZ residues detection.

Keywords: Reduced graphene oxide-silver nanoparticles; poly(L-cys); electrochemical sensors; metronidazole; sensitivity

Introduction

Metronidazole (MNZ) belongs to the nitro-imidazole derivative family, and is used for the treatment of diseases caused by anaerobic bacteria (*Clostridium* and *Bacteroides*) and protozoa (trichomoniasis and amoebiasis) [1]. However, excessive and long-term use of MNZ may also pose a serious hazard for health because of its carcinogenic, mutagenic and genotoxic [2, 3]. It has been reported that MNZ isexcreted into breast milk in large amounts of up to 20% during breastfeeding [4]. Thus, it is important to monitor MNZ residues in milk to ensure food safety.

Several metronidazole detection methods have been developed, encompassing chromatography [5], immunoassays [6, 7] and electrochemical techniques [8, 9]. Chromatographic methods (high-performance liquid chromatography (HPLC) and liquid chromatography–tandem mass spectrometry (LC–MS/MS)) are still the most common quantitative and confirmatory methods for MNZ residues. However, they require complicated pretreatments and skilled operators for use. Immunoassays, *i.e.*, enzyme-linked immunosorbent assay and lateral flow test strip based on antibodies, are high-throughput screening methods for small molecular. Nevertheless, it is difficult to prepare highly sensitive antibodies against MNZ due to its chemicalstructures. A broad specificity monoclonal antibody, 1D5, was prepared with the IC50 value of 500 ng mL^{-1} against MNZ, which was not suitable for establishing highly sensitive method for the detection of MNZ [7]. Because of the nitro group in the structure of MNZ can act as a redox-active center, electrochemical sensors have attracted much attention, owing to high sensitivity, low cost and simple operation [10].Thus, the establishment of a new electrochemical sensor is an effective way to monitor MNZ residues.

To improve performance of bare electrodes, diverse electro-catalysts have been explored as electrode modifiers for the detection of MNZ, such as nickel-manganous oxide nano-crumbs decorated partially reduced graphene oxide [11], N, S, P-Triple Doped Porous Carbon [12], chitosan-pectin polyelectrolyte complex [13], Praseodymium Vanadate-Decorated Sulfur-Doped Carbon Nitride Hybrid Nanocomposite [14], metal-organic framework (type ZIF-67) [15] and so on. Among those nanomaterials, reduced graphene oxide-nanoparticle composites have attracted attention in the electrochemical sensor arena because of their unique physicochemical properties, *i.e.*, large surface area, high electrocatalytic activity, excellent electronic conductivity, and small dimensional size [16]. In addition, among various noble metalnanomaterials (Ag, Au, Pt etc.), Ag is mostly attractive owing to its low cost and small negative environmental impact [17]. Moreover, Ag nanoparticle-reduced graphene oxide (rGO-AgNPs) composites displayed a high oxygen reduction reaction activity via a four-electron transfer pathway as compared to a commercialcarbon-supported Ag catalyst (60 wt.% Ag/C, Premetek) [18]. Also, the rGO-AgNPs nanocomposite exhibited excellent catalytic activity and stability toward the detection of nitrite ions [19] and the reduction of 4-nitrophenol to 4-aminophenol with sodium borohydride [20]. Thus, the rGO-AgNPs nanocomposite modified on electrode could improve the oxygen reduction reaction activity.

Another way to modify electrodes is electropolymerization of amino acids because of their ease of fabrication, ability to form a controllable thin film andpresence of functional groups that help them form multifunctional layers [21, 22]. L-cysteine (L-cys) is a linker agent and weak reductant due to its functional –SH, – NH2 and –COOH groups. It can be easily polymerized to form poly(L-cys) on electrode surfaces using cyclic voltammetry [23, 24]. Gözde Aydoğdu Tığ has used the Au-Ag nanoparticles/poly(L-Cysteine)/reduced graphene oxide nanocomposite for establishing a highly sensitive amperometric biosensor for the determination of NADH and ethanol [21]. Thus, L-cys is electropolymerized on the electrode to form poly(L-cys), which could interact strongly with AgNPs by Ag-S bond to form the stable nanocomposites poly(L-cys)/rGO-AgNPs, further improving the sensitive of the detection.

The aim of this study was developed a new sensitivity electrochemical sensor based on poly(L-cys)/rGO-AgNPs modified the electrode for the detection of MNZ (scheme 1). First, the rGO-AgNPs composites were synthesized via a green "one-pot"method using L-cys as a reducing agent in alkaline media. Subsequently, the rGO-AgNPs composites was dropped on the working electrode, and poly(L-cys)obtained by electropolymerization was synergized with rGO-AgNPs nanocomposites to enhance electrocatalytic effects. The combination of rGO-AgNPs and poly(L-cys) led to increased sensitivity of this electrochemical sensor. Finally, the prepared sensor was successfully used for the MNZ detection by differential pulse voltammetry (DPV).
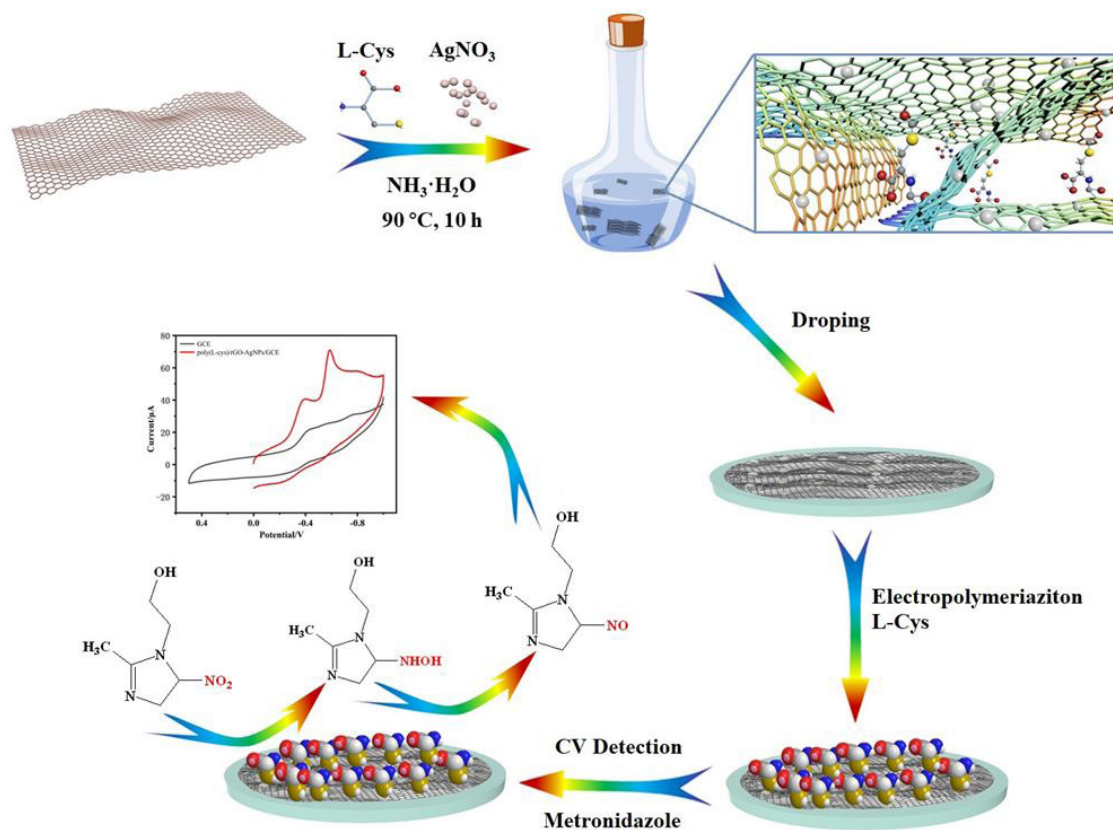
Scheme 1: Synthesis of poly(L-cys)/rGO-AgNPs/GCE and the electrochemical determination of metronidazole

Materials and methods

Reagents and apparatus

Metronidazole, L-cys, and AgNO3 (98%) were purchased from Aladdin (Shanghai, China). GO nanomaterials were generated from previous experiments. Hydrochloric acid (HCl), monosodium phosphate (NaH2PO4), disodium phosphate (Na2HPO4), acetic acid (HAc), sodium hydroxide (NaOH), and ammonia solution (NH3•H2O) were purchased from Sinopharm Chemical Reagent Co. Ltd. (Beijing, China). A stock solution of metronidazole (1 mg mL^{-1}) was prepared in ultrapure water.

All reagents were used without further purification.

Reduced GO-AgNPs composites images were obtained using a field emission transmission electron microscope (FE-TEM, FEI Tecnai G2 F20, MA, USA), operating at 200 kV, and a scanning electron microscope (SEM, Zeiss MERLIN Compact, Germany). UV-vis absorption curves were collected on a Purkinje General T60 UV-Vis spectrophotometer (Beijing Purkinje General Instrument Co. Ltd., China).A chi660e electrochemical workstation (CHI Instrument Co. Ltd., Shanghai, China) was

used for all electrochemical measurements. A conventional three-electrode system was used, including a bare glassy carbon electrode (GCE) (4 mm in diameter) as the working electrode, a saturated calomel electrode (SCE) as the reference electrode, and a platinum wire electrode as the auxiliary electrode.

Synthesis of rGO-AgNPs composites

The disrupted sp^2 hybridization area in GO leads to its poor conductivity, but after reduction, rGO conductivity is recovered due to restored, large delocalized π bonds [25]. Hence, GO must be reduced to generate electrochemical modified materials. In this study, a novel, green method was adopted for the synthesis of rGO-AgNPs using a "one-pot" method. Firstly, a certain amount of GO powder was dispersed in ultrapure water by ultrasonication for 2 h, to generate a homogeneous solution (2 mg mL^{-1}). Secondly, 100 mg L-cys, 100 mg AgNO3 and 400 μL NH3·H 2O(NH3, 25%) were sequentially added to the above (20 mL), under ultrasonication. The mixture was then heated in a water bath at 90°C for 10 h under atmospheric pressure , without stirring. Finally, products were centrifuged (12,000 rpm), washed three times in ultrapure water, and dried at 60°C. The solid powder was prepared at a dispersion of 0.02 mg mL^{-1} in ultrapure water, as an electrode modification material.

Preparation of the electrochemical sensor

Before modification, the bare GCE was polished with a 0.05 mm alumina slurry, and ultrasonicated in absolute ethanol and ultrapure water, respectively. 10 μL of an rGO-AgNPs (0.02 mg mL^{-1}) dispersion was dropped onto the GCE surface, and dried under an infrared lamp. The rGO-AgNPs/GCE assembly was then immersed in 0.02 mg mL^{-1} L-cys solution, and polymerized using cyclic voltammetry (CV) at a potential -0.8 V – 2.2 V for 10 cycles, at a scan rate of 0.1 V s^{-1}. The electrochemical sensor (poly(L-cys)/rGO-AgNPs/GCE) was finally constructed (Scheme 1). All electrochemical measurements were conducted at room temperature (approximately 25°C).

Electrochemical measurements

A certain amount of metronidazole stock solution was added into the cell (volume = 10 mL) containing 5 mL KCl at 0.1 mol L^{-1}. The three-electrode system was then subsequently installed. After an accumulation of 120 s in an open circuit, cyclic voltammograms were measured between -1.0 V–0 V (vs. SCE alone), at a scan rate of 0.10 V s^{-1}. The optimal parameters of differential pulse voltammetry (DPV) parameters were set as increment potential of each point 0.004V, pulse amplitude 0.04V, pulse width 0.05s and pulse period 0.2s. The potential DPV window was set at -0.1 V – -0.4 V. All electrochemical measurements were conducted at room temperature (approximately 25 °C).

Results and discussion

Characterization of rGO-AgNPs composites

The rGO-AgNPs composites are always selected for constructing electrochemical sensors to improve the performance detection due to its higher catalytic effect. Environmentally-friendly reductants, *i.e.*, sodium borohydride [19] and tyrosine [26], were utilized in the synthesis of rGO-AgNPs. Sodium borohydride was a common reductant capable of reducing various functional groups, while it cannot improve the homogeneous dispersion of rGO in solution. Tyrosine as a kind of amino acid containing a hydroxyl group can reduce GO and AgNO3, while it also cannot be regarded as a stabilizer.

In this study, L-cys was considered as a weak reductant to reduce GO and AgNO3 and a linker agent to disperse and immobilize the AgNPs loaded stably on the graphene, and prevent the aggregation of bulk-quantity rGO nanosheets caused by strong π-π stacking in different nanosheets, simultaneously. The rGO-AgNPs nanocomposites were characterized by SEM, TEM, and UV-visible absorption spectroscopy to investigate morphology and nanocomposite interactions. It is seen that abundant AgNPs were successfully loaded on graphene surface (Figure 1A). In addition, AgNPs of relatively uniform particle size (approximately 13.3 nm) were well dispersed on the surface of rGO nanosheets (Figure 1B). As spherical particles possess the lowest surface energies in all volumes, particle interactions were weak [26]. Depending on the mean size of AgNPs obtained from TEM, metal dispersion could be calculated to be 8.4%, demonstrating that AgNPs possessing good catalytic effect, by the equation: D_{Ag} = 5.7/r, where DAg is the metal dispersion of Ag, r is radius of Ag [27]. From high resolution TEM (HTEM) (Figure 1C) and Fast-Fourier transformation of images, the lattice fringe spacing was calculated as 0.233 nm, which was in line with the lattice spacing of Ag (111) diffractive planes reported in other articles [28]. In addition, the UV-visible absorption spectroscopy was also used to investigate nanocomposite interactions. As shown in Figure 1D, rGO-AgNPs nanosheets generated an absorption peak at 270 nm (the red curve), which was characteristic of rGO. When a particular quantity of L-cys was added to the rGO-Ag-NPs solution, the absorption peak at 270 nm disappeared (the black curve), indicating L-cys may have bound with rGO-AgNPs composites via coordinated bonding between AgNPs and –SH. Those results indicated that rGO-AgNPs composites were synthesized successfully.
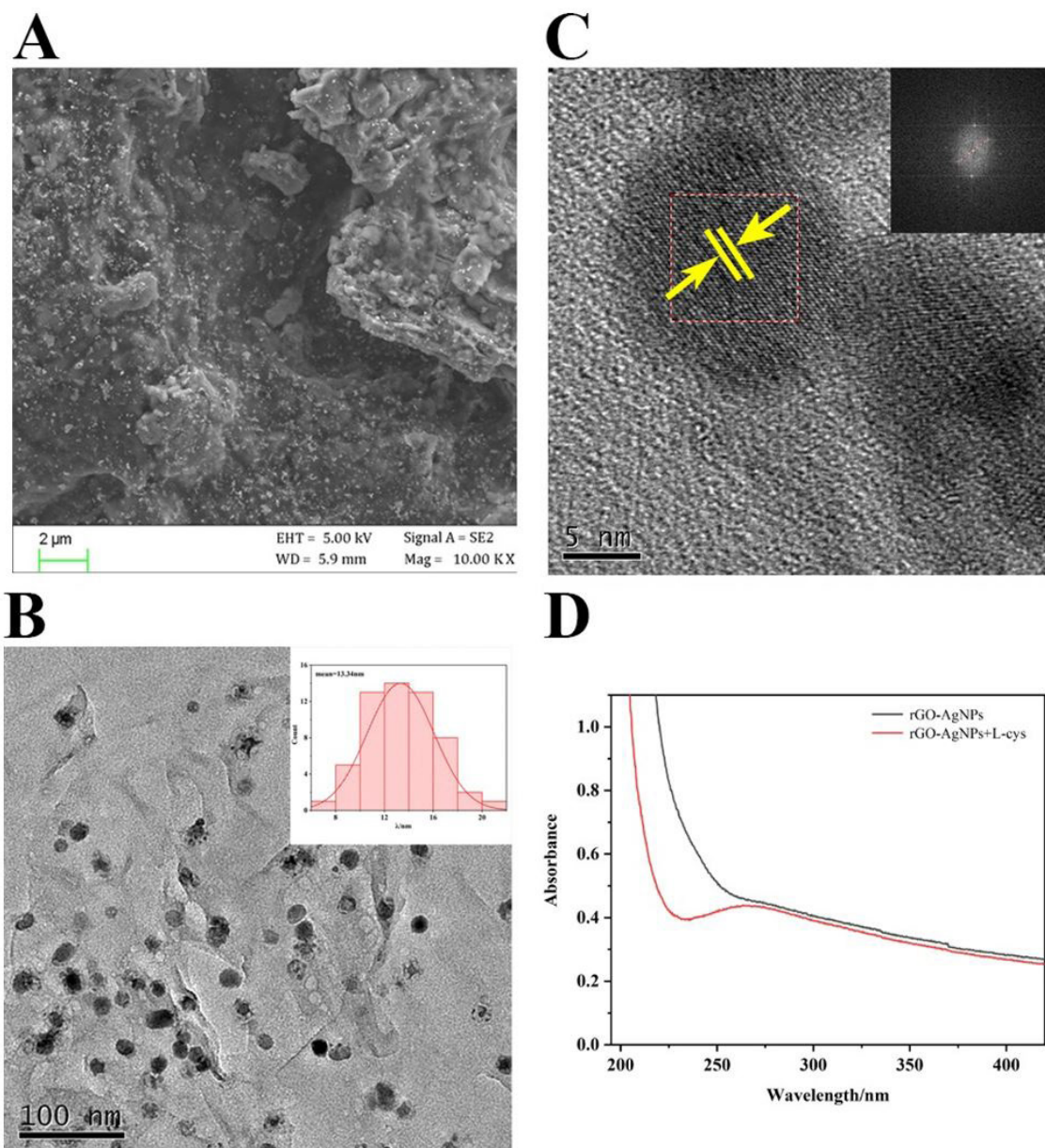
Figure 1: (A) Scanning electron microscope image of rGO-AgNPs at 2μm; (B) Transmission electron microscope images of rGO-AgNPs at 100nm, inset: Size distribution of AgNPs nanoparticles on rGO; (C) High-resolution transmission electron microscope images of AgNPs nanoparticles on rGO at 5nm, inset: Fast-Fourier transformation of high-resolution transmission electron microscope images; (D) UV-vis absorption spectrum of rGO-AgNPs and rGO-AgNPs + L-cys

The electrochemical behavior of metronidazole

CV was used to explore metronidazole (0.02 mg mL^{-1}) responses, against different modified electrodes. MNZ exhibited two weak cathodic peaks (Epc1 occurred at -0.4 V and Epc2 occurred at -0.8 V) on the GCE (Figure 2A). Reduced GO-AgNPs considerably improved the Epc2 cathodic current, with little effect was observed on Epc1. In contrast, poly(L-cys) improved the cathodic peak current and peak potential of Epc1, but weakened the Epc2 peak current. Notably, poly(L-cys) synergized with rGO-AgNPs nanocomposites to further enhance peak currents,

and electro-catalyze the two cathodic peaks have a positive shift. When combined with the calculated effective area (the above data), peak current densities were 80.75 μA cm-2 (peak 1) and 83.13 μA cm-2 (peak 2) for bare GCE, and 126.91 μA cm-2 (peak 1) and 195.31 μA cm-2 (peak 2) for the poly(L-cys)/rGO-Ag-NPs/GCE. Thus, poly(L-cys) in synergizing with rGO-AgNPs nanocomposites not only enhanced signal intensity, but also exerted electrocatalytic effects on the electrochemical behavior of metronidazole. These observations suggested our modified electrode was effective for determining metronidazole.

Figure 2B shows the behavior of metronidazole on poly(L-cys)/rGO-AgNPs/GCE, using successive cyclic scans. Peak currents decreased gradually and tended to be stable, indicating reaction intermediates were adsorbed on the electrode surface. From the second scan, cathodic peak shapes were similar, suggesting intermediates were not electroactive.

Optimization of experimental conditions

Several experimental conditions, such as assay buffer, supporting electrolytes and accumulation time, should affect the analytical performance of the electrochemical sensors. Thus, those conditions were optimized in this study. The metronida-
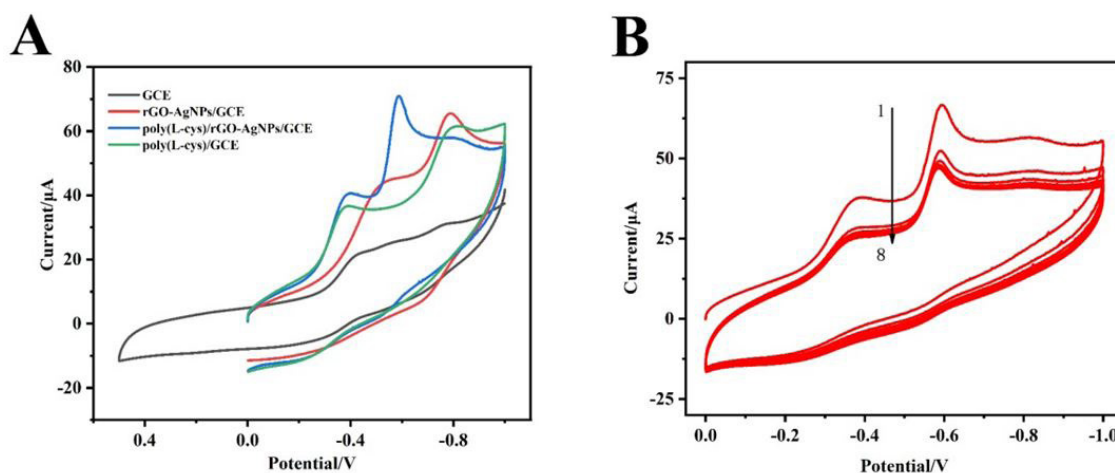

Figure 2: (A) Cyclic voltammetry of GCE, rGO-AgNPs/GCE, poly(L-cys)/GCE and poly(L-cys)/rGO-AgNPs/GCE in 0.02 mg mL-1 metronidazole solution, containing 0.1 mol L−1 KCl. (B) Successive cyclic voltammetry behavior of metronidazole with a concentration of 0.02 mg mL-1 metronidazole solution containing 0.1 mol L−1 KCl. Scan rate: 0.1 V s-1

zole response in KCl (Figure 3A) was similar to NaOH, but metronidazole displayed a better current intensity and shape in KCl. Moreover, supporting electrolytes may exert effects on analytes under aqueous conditions, and similarly affect sensor performance. To address this, we investigated several common laboratory solutions, i.e., H_2SO_4, HCl, HAc, KCl, PBS and NaOH (Figure 3A). Peak currents and shapes were indistinguishable under acidic conditions. A gentle metronidazole peak current was visible for PBS (pH 7), which may have been attributed to the two cathode peaks overlap into one peak due to the slow electron transfer rate of metronidazole on the electrode. The peak potential shifted to the negative with increasing pH for PBS, and peak currents decreased gradually (Figure 3B). The cathodic

peak potential was linear with pH, and the regression equation was expressed as $E_{pc} = -0.044pH - 0.20$ (r = 0.9969) (Inset of figure 3B). The slope representing dE_{pc}/dE_{pH} was 0.044 V pH-1, which was close to 0.059 V pH-1, suggesting that the electrochemical behavior of metronidazole required a stoichiometry of one H+ per one electron. In addition, the effects of adsorption capacity of metronidazole were operated by a serial of accumulation time (Figure 3C) to obtain a higher sensitivity. From 0–4 min, both peak currents (Ipc1 and Ipc2) gradually increased, and then decreased after 2 min (inset of Figure 3C). In a word, KCl, pH 7.0, 2 min of accumulation time were selected as optimum condition for the subsequently experiment.
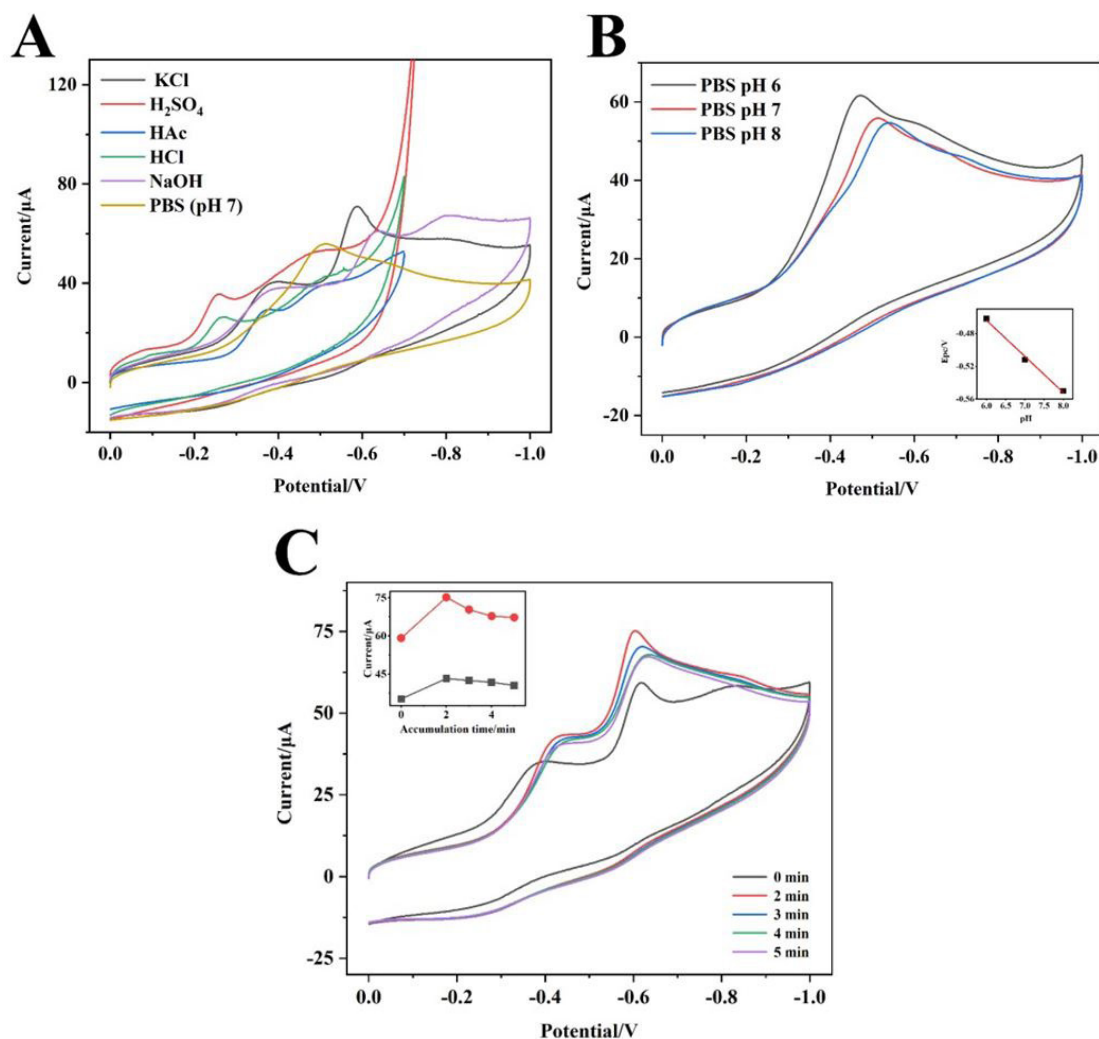
Figure 3: (A) Cyclic voltammetry of metronidazole (0.02 mg mL-1) in KCl, H2SO4, HAc, HCl, NaOH, and PBS (pH 7) (all supporting electrolytes were at 0.1 mol L-1) at the poly(L-cys)/rGO-AgNPs/GCE. (B) Cyclic voltammetry of metronidazole in PBS solutions with different pHs. Inset: a linear regression plot of Epc vs. pH. (C) Influence of accumulation times on poly(L-cys)/rGO-AgNPs/GCE in metronidazole solution (0.02 mg mL-1). Inset: cathodic currents for Epc1 (the black curve) and Epc2 (the red curve)

Investigation of electrochemical sensor performance

In this study, the potassium ferricyanide (K3Fe(CN)6) probe was used to characterize sensor properties. As shown (Figure 4A), the GCE response was a pair of redox peaks using CV method, with a ΔEp (the redox peak potential separation) of 82 mV. After rGO-AgNPs were modified on the electrode, the redox peaks tended to be irreversible, with a ΔEp of 155 mV. Equally, peak currents decreased significantly, suggesting rGO-AgNPs inhibited transfer of Fe(CN)63- onto the electrode interface.

As poly(L-cys) was polymerized on the electrode, the peak current of poly(L-cys)/GCE (ΔEp of 92 mV) was higher than GCE, indicating L-cys promoted the electron transfer of negatively charged Fe(CN)63-. The response signal of poly(L-

Cys)/rGO-AgNPs/GCE (ΔEp of 105 mV) was clearly improved, when compared with rGO-AgNPs/GCE, demonstrating successful construction of the electrochemical sensor.

Electrochemical impedance spectroscopy (EIS) was used to study interfacial properties of modified electrodes. The electron transfer impedance on the electrode surface was equivalent to the curvature radius [29] of the impedance curve in the high frequency region, while the straight linear, low frequency region, was dominated by mass transfer of the probe ([Fe(CN)6]3−/4−). The electron transfer resistance, which presents as the semicircular part, displays the interfacial electron transferring impedance of the probe at the electrode surface. From the superposition chart (Figure 4B), the Nyquist GCE curve generated a very small semicircle in the high frequency

region. When rGO-AgNPs were modified on GCE, the modified electrode Nyquist curve was increased in the semicircle of the high frequency region, when compared with GCE alone, suggesting that rGO-AgNPs/GCE may have blocked electron transfer efficiency. The poly(L-cys)/rGO-AgNPs/GCE Nyquist curve displayed a larger semicircle than rGO-AgNPs/GCE in the high frequency region. These data suggested that associations possibly existed between rGO-AgNPs and L-cys, indicating indirect synergistic effects between the two, and sharply increasing electron transfer resistance. Thus, L-cys and rGO-AgNPs nanomaterials were successfully modified on the electrode.

A chronocoulometry procedure was also performed to determine the effective electrode area in 1 mol L-1 KCl solution, containing 1.0 mmol L-1 K3Fe(CN)6 (Figure 4C). The diffusion coefficient was 7.6×10^{-6} cm2 s-1 [30]. It can be calculated the effective electrode area according to the Anson equation [31] (Equation 1):

$$Q = \frac{2nFAc\left(Dt\right)^{1/2}}{\pi^{1/2}} + Q_{dl} + Q_{ads} \qquad \text{(Equation 1)}$$
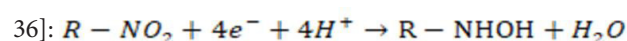
where n = the number of electrons transferred in the analyte. F = the Faraday constant. A = the surface area of the working electrode, and c = the substrate concentration. D = the diffusion coefficient. Qdl = the double-layer charge, and Qads = the Faradaic charge. Depending on the slope of the linear regression Q ~ t1/2, the effective area of the bare electrode, and the modified electrode was 0.040 cm2 and 0.162 cm2, respectively. This demonstrated that poly(L-cys) and rGO-AgNPs increased the effective area and enhanced signal intensity.

To determine the reaction form of metronidazole on the electrode, measurements were performed using serial scan rates (Figure 4D). Both cathodic peak currents (Ipc1 and Ipc2) increased linearly with increasing scan rates. Their regression equations were Ipc1 = 151.51v + 21.71 (Ipc1 = μA, ν = V s-1,
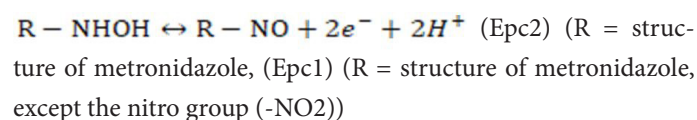
and r = 0.9912) and Ipc2 = 260.28ν + 37.49 (Ipc2 = μA, ν = V s-1, and r = 0.9893), respectively. Additionally, logIpc was proportional to logv, and equations were expressed as log(Ipc1) = 0.48logv + 2.06 (Ipc1 = μA, ν = V s-1, and r = 0.9939) and log(Ipc2) = 0.48logv + 2.30 (Ipc2 = μA, ν = V s-1, and r = 0.9934). The slopes of both curves were approximately 0.5, suggesting the electrochemical behavior of metronidazole was controlled by a mixed diffusion and adsorption system [32].

Based on Laviron theory [33], the number of electrons transferred of irreversible adsorbed system can be expressed as follow (Equation 2):

Where Epc = cathodic peak potential, E0 = standard cathodic peak potential, n = the number of transferred electrons, α = the charge transfer coefficient, F = the Faraday constant, T = the test temperature, ks = the apparent electron-transfer rate constant, and ν = the scan rate. The two cathodic peak potentials were linearly related to lnν, respectively, with regression equations of Epc1 = − 0.43 − 0.021lnν ((Epc1 = V, ν = V s-1,r = 0.9878) and Epc2 = − 0.62 − 0.014lnν (Epc2 = V, ν = V s-1, r = 0.9863). Hence, αn was calculated from the slope; αn1 = 1.2 and αn2 = 1.8. On account of the irreversible electrode process, α was assumed to be 0.5 [34], n1 was approximately 2 and n2 was approximately 4. Considering a stoichiometry of one H+ per one electron, the electrochemical processing of metronidazole generated six electrons and six H+ reactions. The proposed reaction mechanism is summarized below, and accounts for the electrochemical reduction of nitroaromatic compounds [9, 35, 36]:

36]: $R - NO_2 + 4e^- + 4H^+ \rightarrow R - NHOH + H_2O$

except the nitro group (-NO2))

$R - NHOH \leftrightarrow R - NO + 2e^- + 2H^+$ (Epc2) (R = structure of metronidazole, (Epc1) (R = structure of metronidazole, except the nitro group (-NO2))

$$E_{pc} = E^0 - (RT/\alpha nF)\ln(RTk_s/\alpha nF) + (RT/\alpha nF)\ln v \qquad \text{(Equation 2)}$$
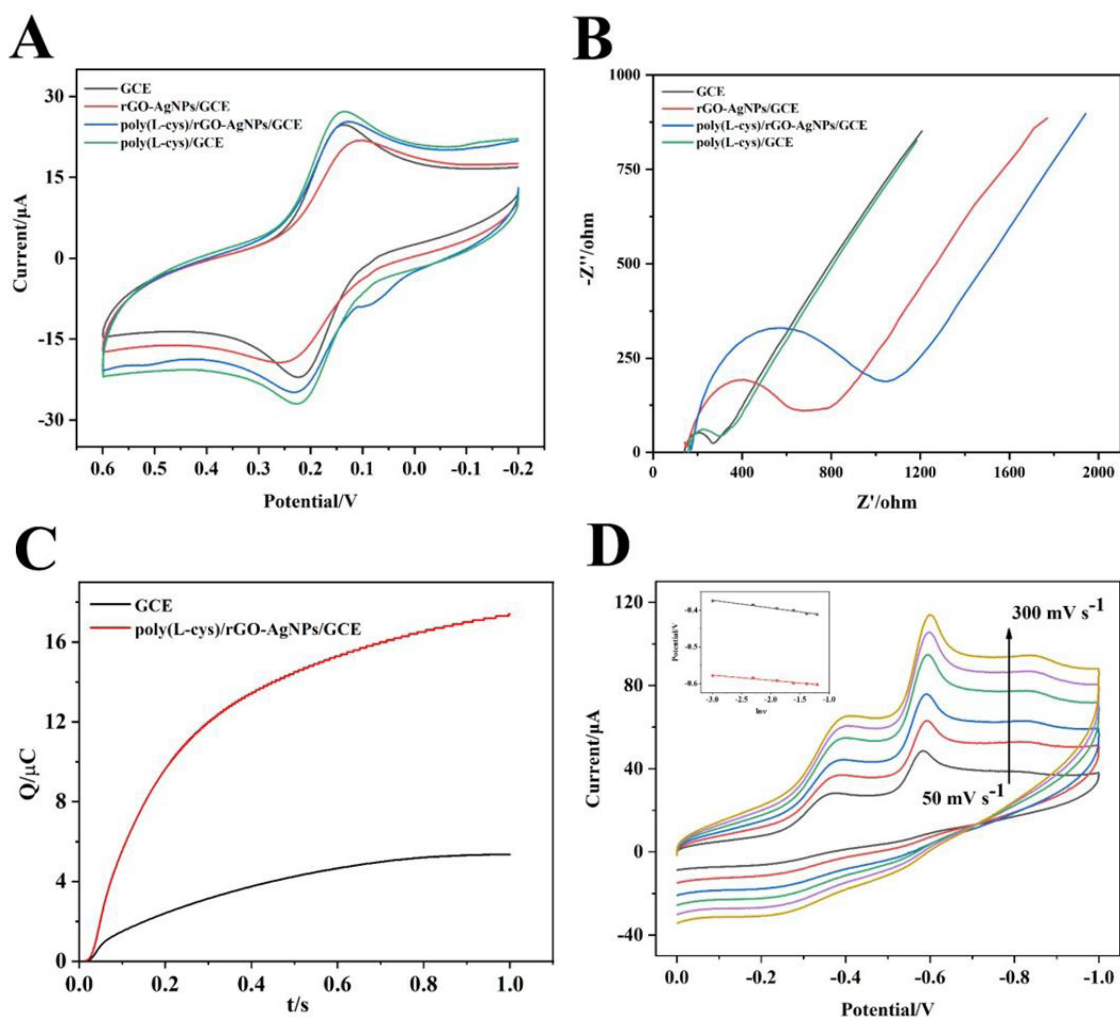
Figure 4: (A) Cyclic voltammetry of GCE, rGO-AgNPs/GCE, poly(L-Cys)/GCE, and poly(L-cys)/rGO-AgNPs/GCE in 1.0 mmol L-1 K3[Fe(CN)6]. (B) Electrochemical impedance spectroscopy of GCE, rGO-AgNPs/GCE, poly(L-cys)/GCE and poly(L-cys)/ rGO-Ag-NPs/GCE in 5.0 mmol L−1 K3[Fe(CN)6]/K4[Fe(CN)6] containing 0.1 mol L−1 KCl. (C) Chronocoulometry of GCE and poly(L-cys)/rGO-AgNPs/GCE in 1.0 mmol L−1 K3[Fe(CN)6], containing 1 mol L−1 KCl. (D) Cyclic voltammetry of metronidazole (0.02 mg mL-1) on poly(L-cys)/rGO-AgNPs/GCE at different scan rates: i.e. 50–300 mV s-1. Inset: linear regression plot of Epc1 (or Epc2) vs. lnv

Quantitative determination of metronidazole by DPV

DPV was quantitatively applied due to its high sensitivity under optimal parameters (DPV scans ranged from -0.4V – -1.0V, with an increment of 0.006 V, a pulse period of 0.2 s, a muplitude of 0.04 V, a pulse width of 0.05 s, and a standing time of 2 s). A wide metronidazole concentration range of 2 µg L⁻¹– 100,000 µg L⁻¹ was used to determine a linear range. As shown in Figure 5, the linear of cathodic peak currents were ranged from 2 µg L-1 to 80,000 µg L⁻¹. The linear regression equation (upper inset of Figure 5) was Ipc = (667.62±26.79)c + (3.58±0.54)) (Ipc = µA, c = mg mL⁻¹, and r = 0.9954), with a limit of detection (LOD) of 0.4 ng mL⁻¹ estimated by a signal to noise (S/N) ratio of 3. When compared with other electrochemical methods (from the past three years), our sensor possessed a wider linear range, and a considerably lower limit of detection compared with other electrochemical sensors (Table 1). Although, the LOD value is not as good as that of NiMnO@pr-GO/GCE [11], the present study possesses a wider linear range.
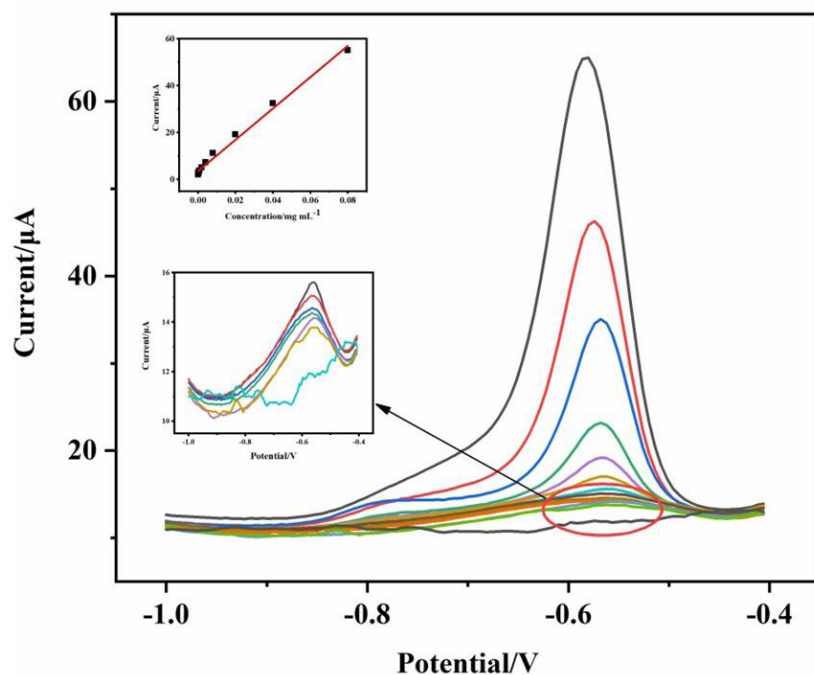
Figure 5: DPV characterization of metronidazole at different concentrations: i.e., 0, 2×10-6, 8×10-6, 8×10-5, 2×10-4, 4×10-4, 8×10-4, 2×10-3, 4×10-3, 8×10-3, 2×10-2, 4×10-2, and 8×10-2 mg mL-1. Inset: calibration curve and peak currents of poly(L-cys)/rGO-AgNPs/GCE in KCl (0.1 mol L-1) and the magnifying superposed DPV i-Epc curves for low concentrations (0, 2×10-6, 8×10-6, 8×10-5, 2×10-4, 4×10-4, 8×10-4 mg mL-1). upper inset: the linear regression equation between concentration of metronidazole and Ipc. Bottom inset: the larger version of curves in lower concentrations

Table 1: Comparison of the present method and other reported electrochemicalmethods for determination of metronidazole in recent three years

Electrochemical sensors	Electrochemi-calmethods	Linear ranges ($\mu mol \, L^{-1}$)	Limit of detection($nmol \, L^{-1}$)	Reference
CuCo2O4/N-CNTs/MIP/GCE	DPV	0.005-0.1, 0.1-100	0.48	[8] Wang et al, 2019
NiMnO@pr-GO/GCE	DPV	0.1-234	0.09	[11] Vivekanandan et al. 2020
NSP-PC/GCE	LSV	0.1-45, 50-350	13	[12] Yalikun et al., 2019
CS-PC BPE/GCE	DPV	0.01-465	9	[13] Ranganathan et al. 2019
PrV/SCN/GCE	Amperometry	0.001-2444	0.8	[14] Kokulnathan and Chen 2019
ZIF-67C@rGO/GCE	DPV	0.5-1000	50	[15] Chen et al. 2019
O-gCN/GCE	DPV	0.01-2060	5	[36] Kesavan et al. 2021
C60-rGO-NF/SPE	SWV	0.5-34.0	35	[37] Materón et al. 2021
poly(L-Cys)/rGO-AgNPs/GCE	DPV	0.012-460	2.3	This work

Reproducibility, repeatability, stability and interference

The practical application of poly(L-cys)/rGO-AgNPs/GCE was estimated using reproducibility, repeatability, stability and interference measurements. The relative standard deviation (RSD) of cathodic peak currents, for five successive tests was 1.5 % in metronidazole solution. After the bare GCE was polished and modified three times respectively, the RSD was 4.6%. The sensors also possessed a detection capability of 87% after 14 days storage at 4 °C. Potential interfering molecules in real samples were evaluated to assess the anti-interference ability of the modified electrode. The tolerance limit was < 10% of the relative error, in 200-fold concentrations of Al^{3+}, Fe^{3+}, Zn^{2+}, NO_3^-, and SO_4^{2-}, and in 100-fold concentrations of glucose, ascorbic acid, citric acid and sucrose.

Sample application

To test sensor applicability in real samples, a standard addition method was used to detect metronidazole in milk. Specifically, the samples did not require complicated pretreatment, such as centrifuged and filtered, but only needed to be diluted with KCl solution (0.1 mol L-1) (1:1). The appropriate amount of metronidazole stock solution was added into the above dilution and measured. As shown in Table 2, the recoveries were ranged from 88.4% to 106.8% with RSD below 5.1%.

Table 2: Recovery of the determination of MNZ in milk samples (n=5)

Spiked (μg L^{-1})	Found (μg L^{-1})	Recovery (%)	RSD (%)
50	44.2	88.4	4.8
100	94.5	94.5	5.1
1000	106.8	106.8	3.4

Conclusions

In this study, a highly sensitive electrochemical sensor based on poly(L-cys)/rGO-AgNPs modified GCE was developed for rapid detection of MNZ with a LOD value of 0.4 ng mL-1 in milk sample. The recovery was ranged from 88.4% to 106.8% with RSD below 5.1% for the determination of MNZ in milk samples.

However, the limitation of stability of the nanocomposites on the electrode remains to be resolved. In the future, the formation of chemical bonds between the electrode surface and rGO can be explored to improve the limitation of stability to increase the service life of the electrochemical sensors and increase the sensitivity. In addition, the sensor reported here demonstrated high potential for MNZ residue determination in biological matrix applications, and could be expanded to other target analytes.

Conflict of Interest

All the authors declare that they have no known competing financial interests or personal relationships that could have appeared to influence the work reported in this paper.

References

1. CW Ang, AM Jarrad, MA Copper, MAT Blaskovich (2017) Nitroimidazoles: Molecular fireworks that combat a broad spectrum of infectious diseases. J Med Chem 60: 7636.

2. JS Walsh, GT Miwa (2011) Bioactivation of drugs: risk and drug design. Annu Rev Pharmacol Toxicol 51: 145.

3. S Patterson, S Wyllie (2014) Nitro drugs for the treatment of trypansomatid diseases: past, present, and future prospects. Trends Parasitol 30: 289.

4. T Kokulnathan, SM Chen (2019) Praseodymium vanadate decorated sulfur-doped carbon nitride hybrid nanocomposite: the role of synergistic electrocatalyst for the detection of metronidazole. ACS Appl Mater Interfaces 11: 7893.

5. SL Stancil, L Haandel, S Abdel-Rahman, RE Pearce (2018) Development of a UPLC-MS/MS method for quantitation of metronidazole and 2-hydroxy metronidazole in human plasma and its application to a pharmacokinetic study. J Chromatogr B 1092: 272.

6. Y Wang, F He, Y Wan, M Meng, J Xu, Y Zhang, J Yi, C Feng, S Wang, R Xi (2011) Indirect competitive enzyme-linked immuno-sorbent assay (ELISA) for nitroimidazoles in food products. Food Addit Contam 28: 619.

7. W Han, Y Pan, Y Wang, D Chen, Z Liu, Q Zhou, L Feng, D Peng, Z Yuan (2016) Development of a monoclonal antibody-based indirect competitive enzyme-linked immunosorbent assay for nitroimidazoles in edible animal tissues and feeds. J Pharmaceut Biomed 120: 84.

8. Y Wang, L Yao, X Liu, J Cheng, W Liu, T Liu, M Sun, L Zhao, F Ding, Z Lu, P Zou, X Wang, Q Zhao, H Rao (2019) CuCo2O4/N-Doped CNTs loaded with molecularly imprinted polymer for electrochemical sensor: Preparation, characterization and detection of metronidazole. Biosens Bioelectron 142: 111483.

9. AA Ensafi, P Nasr-Esfahani, B Rezaei (2018) Metronidazole determination with an extremely sensitive and selective electrochemical sensor based on graphene nanoplatelets and molecularly imprinted polymers on graphene quantum dots. Sens Actuators B: Chem 270: 192.

10. RKA Amali, HN Lim, I Ibrahim, NM Huang, Z Zainal, SAA Ahmad (2021) Significance of nanomaterials in electrochemical sensors for nitrate detection: A review. Trends Environ Anal Chem 31: e00135.

11. AK Vivekanandan, SV Selvi, S Chen, SH Chen (2020) Sonochemical synthesis of nickel-manganous oxide nanocrumbs decorated partially reduced graphene oxide for efficient electrochemical reduction of metronidazole. Ultrason Sonochem 68: 105176.

12. N Yalikun, X Mamat, Y Li, X Hu, P Wang, G Hu (2019) N, S, P-triple doped porous carbon as an improved electrochemical sensor for metronidazole determination. J Electrochem Soc 166: B1131.

13. P Ranganathan, B Mutharani, S Chen, P Sireesha (2019) Biocompatible chitosan-pectin polyelectrolyte complex for simultaneous electrochemical determination of metronidazole and metribuzin. Carbohyd Polym 214: 317.

14. T Kokulnathan, SM Chen (2019) Praseodymium vanadate-decorated sulfur-doped carbon nitride hybrid nanocomposite: The role of a synergistic electrocatalyst for the detection of metronidazole. ACS Appl Mater Inter 11: 7893.

15. H Chen, X Wu, R Zhao, Z Zheng, Q Yuan, Z Dong, W Gan (2019) Preparation of reduced graphite oxide loaded with cobalt (II) and nitrogen co-doped carbon polyhedrons from a metal-organic framework (type ZIF-67), and its application to electrochemical determination of metronidazole. Microchim. Acta 186: 623.

16. A Ambrosi, CK Chua, A Bonanni, M Purnera (2014) Electrochemistry of graphene and related materials. Chem Rev 114: 7150.

17. S Liu, L Wang, J Tian, Y Luo, X Zhang, X Sun (2011) Aniline as a dispersing and stabilizing agent for reduced graphene oxide and its subsequent decoration with Ag nanoparticles for enzymeless hydrogen peroxide detection. J Colloid Interface Sci 363: 615.

18. EJ Lim, SM Choi, MH Seo, Y Kim, S Lee, WB Kim (2013) Highly dispersed Ag nanoparticles on nanosheets of reduced graphene oxide for oxygen reduction reaction in alkaline media. Electrochem Commun 28: 100.

19. NI Ikhsan, P Rameshkumar, A Pandikumar, MM Shahid, NM Huang, SV Kumar, HN Lim (2015) Facile synthesis of graphene oxide–silver nanocomposite and its modified electrode for enhanced electrochemical detection of nitrite ions. Talanta 144: 908.

20. KC Hsu, DH Chen (2014) Green synthesis and synergistic catalytic effect of Ag/reduced graphene oxide nanocomposite. Nanoscale Res Lett 9: 484.

21. GA Tığ (2017) Highly sensitive amperometric biosensor for determination of NADH and ethanol based on Au-Ag nanoparticles/poly(L-Cysteine)/reduced graphene oxide nanocomposite. Talanta 175: 382.

22. D Zhang, L Li, W Ma, X Chen, Y Zhang (2017) Electrodeposited reduced graphene oxide incorporating polymerization of L-lysine on electrode surface and its application in simultaneous electrochemical determination of ascorbic acid, dopamine and uric acid. Mater Sci Eng C 70: 241.

23. B Hatamluyi, F Lorestani, Z Es'haghi (2018) Au/Pd@rGO nanocomposite decorated with poly (L-Cysteine) as a probe for simultaneous sensitive electrochemical determination of anticancer drugs, Ifosfamide and Etoposide. Biosens Bioelectron 120: 22.

24. M Hasanzadeh, HN Baghban, N Shadjou, A Mokhtarzadeh (2018) Ultrasensitive electrochemical immunosensing of tumor suppressor protein p53 in unprocessed human plasma and cell lysates using a novel nanocomposite based on poly-cysteine/graphene quantum dots/gold nanoparticles. Int J Biol Macromol 107: 1348.

25. Istrate, O. M.; Rotariu, L.; Bala, C. Electrochemical determination of NADH using screen printed carbon electrodes modified with reduced graphene oxide and poly(allyamine hudrochloride). Microchim. Acta 2016, 183, 57-65.

26. SB Maddinedi, BK Mandal, NK Fazlur-Rahman (2017) High reduction of 4-nitrophenol using reduced graphene oxide/Ag synthesized with tyrosine. Environ Chem Lett 15: 467.

27. JR Anderson (1975) Structure of Metallic Catalysts. Academic Press, London, New York, San Francisco, pp469.

28. R Zhou, Y Yin, D Long, J Cui, H Yan, W Liu, JH Pan (2019) PVP-assisted laser ablation growth of Ag nanocubes anchored on reduced graphene oxide (rGO) for efficient photocatalytic CO2 reduction. Prog Nat Sci Mater 29: 660.

29. Y Mao, Q Fan, J Li, L Yu, L Qu (2014) A novel and green CTAB-functionalized graphene nanosheets electrochemical sensor for Sudan I determination. Sens Actuators B: Chem 203: 759.

30. L Yu, Y Mao, Y Gao, L Qu (2014) Sensitive and simple voltametric detection of Sudan I by using platinum nanoparticle-modified glassy carbon electrode in food samples. Food Anal Methods 7: 1179.

31. F Anson (1964) Application of potentiostatic current integration to the study of the adsorption of cobalt (III)-(ethylenedinitrilo(tetraacetate)) on mercury electrodes. Anal Chem 36: 932.

32. L Yu, Y Mao, L Qu (2013) Simple voltametric determination of Rhodamine B by using the glassy carbon electrode in fruit juice and preserved fruit. Food Anal Methods 6: 1665.

33. E Laviron (1979) General expression of the linear potential sweep voltammogram in the case of diffusionless electrochemical systems. J Electroanal Chem 101: 19.

34. AJ Bard, LR Faulkner (2001) Electrochemical Methods Fundamentals and Applications. John Wiley & Sons, Inc., New York, 2001, Chapter 3.

35. HB Ammar, MB Brahim, R Abdelhédi, Y Samet (2016) Boron doped diamond sensor for sensitive determination of metronidazole: Mechanistic and analytical study by cyclic voltammetry and square wave voltammetry. Mater Sci Eng C 59: 604.

36. G Kesavan, V Vinothkumar, SM Chen, TD Thangadurai (2021) Construction of metal-free oxygen-doped graphitic carbon nitride as an electrochemical sensing platform for determination of antimicrobial drug metronidazole. Appl Surf Sci 556: 149814.

37. EM Materón, A Wong, TA Freitas, RC Faria, ON Oliveira (2021) A sensitive electrochemical detection of metronidazole in synthetic serum and urine samples using low-cost screen-printed electrodes modified with reduced graphene oxide and C60. J Pharm Anal 11: 646.